

Dynamic Behaviors of Lipid-Like Self-Assembling Peptide A₆D and A₆K Nanotubes

Aki Nagai¹, Yusuke Nagai^{1,2}, Hongjing Qu, and Shuguang Zhang^{1,*}

¹Center for Biomedical Engineering NE47-379, Massachusetts Institute of Technology,
77 Massachusetts Avenue, Cambridge, MA 02139-4307, USA

²Menicon Co. Ltd., 5-1-10 Takamori-dai, Kasugai, Aichi 487-0032, Japan

Nanoscience and nanotechnology require development of nanomaterials that are amiable for molecular design from bottom up. Molecular designer self-assembling peptides are one of such nanomaterials that will become increasingly important for the endeavor. Peptides have not only been used in all aspects of biomedical and pharmaceutical research and medical products, but also have had enormous impact in nascent field of designed biological materials. We here report the dynamic structures of lipid-like designer peptide A₆D (AAAAAAD) and A₆K (AAAAAAK) that undergo self-assembly into nanotubes in water and salt solution. We not only analyzed their self-assemblies using dynamic light scattering to determine the critical aggregation concentration (CAC), but also use atomic force microscope to observe their nanostructures. We also propose a simple scheme by which these lipid-like peptides self-assemble into dynamic nanostructures. Since the knowledge of CAC is important for uses of these peptides for a variety of applications, these findings may have significant implications in the study of molecular self-assembly and for a wide range of utilities of designer self-assembling peptide materials.

Keywords:

Biological building blocks including peptides and proteins,^{1–11} diacylenic lipids,^{12–14} have recently been employed to design and fabricate for a wide range of nanoscale materials for diverse applications. The designed peptide nanomaterials offer unique material engineering opportunities because of their relatively simple structures and easy scale up commercial productions. Different types of nanomaterials have been developed using various classes of self-assembling peptides. These include peptide nanofibers,^{3, 6–10, 15–19} peptide nanocoatings,^{11, 20} peptide scaffolds,^{7–10, 15–19} and peptide nanotubes.^{21–27} The peptide nanotubes are of special interest for their potential utilities as drug and gene delivery vehicles, scaffold for coating metal nanowires, and artificial transmembrane channel, surfactants for stabilization of membrane proteins.^{4–5, 25–27}

The molecular self-assembly of peptide nanotubes is facilitated through weak, non-covalent bonds: notably hydrogen bonds, ionic bonds (electrostatic interactions), hydrophobic interactions, van der Waals interactions and water-mediated hydrogen bonds.¹

We previously reported a new class of lipid-like peptides, also called peptide surfactants^{21–24} that can spontaneously undergo self-assembly to form dynamic nanostructures in pure solution, similar as other lipids and surfactants. These lipid-like peptides were designed with a head group of one or two hydrophilic amino acids, either positively charged residues lysine, arginine or histidine, or negatively charged residues aspartic acid or glutamic acid; and a tail of four or more consecutive hydrophobic amino acids, such as glycine, alanine, valine, isoleucine, leucine, phenylalanine, tyrosine, and tryptophan. In aqueous solutions at a certain pH without other membrane proteins, these lipid-like peptides have a tendency to sequester their hydrophobic tails to self-organize themselves into highly ordered nanotube structures. These nanotube structures have been observed by transmission electron microscopy (TEM) using quick-freeze/deep-etch sample preparation methods.^{21–24} The size distributions of the nanostructures became broader over time, suggesting a very dynamic process of self-assembly and disassembly.²¹ It is likely that the peptides and their assemblies change over time. Since the chemical property of the lipid-like peptides are similar to some lipids and surfactants that are very important for stabilize membrane proteins. Thus, our study may not only

*Author to whom correspondence should be addressed.

gain insight into the dynamics of lipid-like self-assembling peptides, but also find application for studying structure and function of diverse membrane proteins.

It is estimated that about one third of total genes in the all sequenced genomes of organisms code for membrane proteins.^{28–29} This fact reflects the vital roles membrane proteins in the function of living systems. Membrane proteins involve in a wide spectrum of essential functions including convert energy in photosynthesis, sense their environments in signal transduction, transport molecules in and outside of cells, and communicate with their surroundings. Furthermore, many metabolic enzymes including energy producing proteins and protein complexes are embedded in lipid membrane. Yet, little is known about majority of their structures, nor the detailed mechanisms of their functions. Although ~35,000 three-dimensional protein structures have been elucidated (August 2006) only 218 (114 unique ones) of these are of membrane proteins. This disparity stems from the technical challenge of solubilizing, stabilizing, and crystallizing proteins that are membrane-bound, particularly integral membrane proteins. Considerable efforts have been made to solubilize, stabilize, and crystallize membrane proteins using diverse lipid-like peptides. Our lipid-like peptides may be useful for these studies.

We have shown that these short lipid-like amphiphilic peptides could solubilize and stabilize various membrane proteins and membrane protein complexes.^{30–32} For negatively charged head group, the C-terminal end of the peptide is uncapped and thus carries its inherent negatively charged carboxylic acid group. Therefore aspartic acid based amphiphilic peptides, such as A₆D consisting of six alanines (A) followed by a negatively charged aspartic acid (D), carry a maximum of -2 charge at a pH above the pK_a's of the carboxylic acids (pK_a ~ 3.7), one from the C-terminus and one from the side chain of aspartic acid. On the other hand, A₆K has a lysine with a positively charged head. The pK_a of lysine side chain is ~10, at neutral pH, it bears a net positive charge.

Similar to common surfactants such as dodecyl maltoside (DM) and octyl glucoside (OG), this class of lipid-like peptides can stabilize the functions of membrane proteins outside of the natural cellular membrane. Lipid-like peptides, however, may have different stabilizing mechanism than common surfactants with alkane tails. They may interact proteins through intermolecular hydrogen bonding between the peptides and protein molecules themselves.

When using surfactants to stabilize membrane proteins, it is important to know the critical aggregation concentration (CAC), also commonly referred to as the critical micelle concentration (CMC), a value at which the energetically favorable release of water molecules around the hydrophobic region(s) of the surfactants become more significant than the electrostatic repulsion of the head groups, causing the molecules to self-assemble into micelles and

other ordered structures. The types of structures formed depend on many different factors, such as the shape of the monomers and chemical property of these molecule. Solubilization and stabilization of membrane proteins are usually conducted at or slightly above the CAC of the surfactants. This allows for the membrane proteins to be solubilized inside the pre-formed micelles. Concentrations significantly higher than the CAC are usually not used as these surfactants may also interfere with membrane protein structures.

In order to understand how the lipid-like peptides self-assemble in water and in PBS, we carried out experiments to elucidate their behavior. We here report the measurement of critical aggregate concentrations (CAC's) of 2 lipid-like peptides, A₆D and A₆K and correlate them to structural behaviors. These results are essential so as to use these lipid-like peptides for stabilization studies of membrane proteins.

1. MATERIALS AND METHODS

1.1. Peptide Design and Preparation

The lipid-like peptides have a hydrophilic head and a hydrophobic tail. The hydrophobic tail's length was adjusted to approximately phospholipids size. The hydrophilic head can be chosen from anionic or cationic amino acids. Two kinds of lipid-like peptides were chosen with good solubility in neutral water. Ac-AAAAAAD (A₆D) and Ac-AAAAAAK-CONH₂ (A₆K) hydrophobic tails consist of six alanine residues and hydrophilic head, which is either an aspartic acid or a lysine. A₆D has aspartic acid with two negative charges at pH 7. A₆K has lysine head with positive charge at pH 7.

These peptides were commercially synthesized by Synpep, Dublin, CA or Synthetech, Albany, OR (www.synthetech.com). These peptides were solubilized in sterile water to a concentration of 12 mM, and their pH values were neutralized with 1 N NaOH in centrifuge tubes. The solutions were sonicated for 30 minutes in an Aquasonic Model 50HT water bath (VWR Scientific). These concentrated solutions were diluted to each concentration by adding Milli-Q water, or 1 × Phosphate Buffered Saline Buffer (100 mM KH₂PO₄, 10 mM Na₂HPO₄, 137 mM NaCl, 2.7 mM KCl, pH 7.4, Roche Diagnostics, Indianapolis, IN). The peptide solutions in serial dilutions were sonicated for 30 minutes at each concentration, and kept overnight at room temperature before dynamic light scattering measurements and atomic force microscopy measurements.

1.2. Dynamic Light Scattering (DLS)

An aliquot of 200 μ l of the peptide solution in various concentrations was used to perform DLS experiments using PDDLs/Batch (Precision Detectors, Franklin, MA). The

scattered light was collected at a 90° angle and the number of the photons falling on an avalanche photodiode was detected as the intensity of scattered light. Data was acquired and displayed by Precision Deconvolve program. These experiments were repeated three times.

1.3. Atomic Force Microscopy (AFM)

For AFM experiments, 2 μl sample was immediately deposited onto a freshly cleaved mica surface. Each aliquot was left on mica for 30 seconds, and rinsed with 200 μl of Milli-Q water. The peptide sample on the mica surface was then air-dried, and images were acquired immediately. The images were obtained by scanning the mica surface in air under ambient conditions using an AFM (Nanoscope IIIa, Digital Instruments, Santa Barbara, CA) operated in tapping mode. Soft silicon cantilevers were chosen (FESP, Veeco Probes). AFM scans were taken at 512 × 512-pixels resolution and produced topographic images of the samples in which the brightness of features increases as a function of height. Typical scanning parameters were as follows: tapping frequency 60 kHz, RMS amplitude before engage 1–1.2 V, integral and proportional gains 0.2–0.6 and 0.4–1.2, respectively, set point 0.7–1.0 V, and scanning speed 1–1.5 Hz. These experiments were repeated three times.

2. RESULTS AND DISCUSSION

2.1. Designer Lipid-Like Peptides

The lipid-like peptides were molecular-designed to mimic amphiphilic lipid molecules ~2–3 nm with a hydrophilic head and a hydrophobic tail. We chose two kinds of peptides, one has an anionic head, aspartic acid A₆D, and the other has a cationic head lysine A₆K (Fig. 1). A₆D has two negative charge in solution >pH 3.7 (Fig. 2) which is the dissociation constant of aspartic acid's -COOH. A₆K has one positive charge on its side chain below pH 10. The peptide solutions were adjusted to pH 7. 12 mM of peptide solutions in water were clear without noticeable precipitations. Aliquots of 0.01 mM to 3 mM of diluted solutions were prepared to carry out DLS experiments.

They were also diluted by adding 1 × PBS, although high concentration solutions in PBS which were over 4 mM become cloudy indicating the partial insolubility. The same peptide solutions in PBS were used for both DLS measurement and AFM scanning.

The cationic lipid-like peptide, A₆K (AAAAAAK), has a head with a positively charged lysine and a hydrophobic tail of six alanines. Under neutral pH and below the lysine pKa 10 (Fig. 2), its population bears positive charge in aqueous solution. We used AFM and dynamic light scattering to study the relationship of the changes in dynamic behavior of the nanostructures to further our understanding of the lipid-like peptide self-assembly.

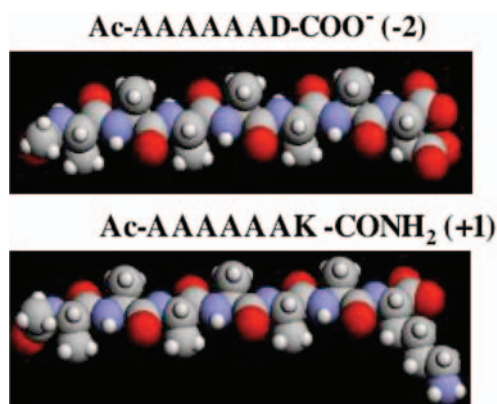


Fig. 1. Molecular models of the lipid-like peptides: A₆D and A₆K. The peptides consist of hydrophobic tail of six alanine residues and a hydrophilic head, either aspartic acid or lysine. The peptides are approximately 2.5 nm in length. The C terminus of A₆D bears two negative charges of two carbonic acids, one from a side chain of D and another from the non-capped C terminus. A₆K bears one positive charge of one amine from a side chain of K (lysine). The color code: carbon, gray; nitrogen, blue; oxygen, red; hydrogen, white.

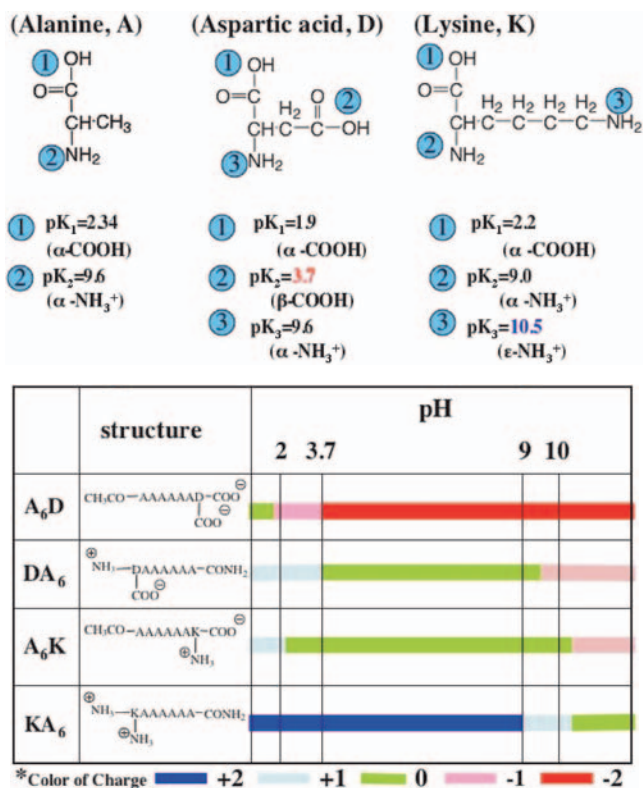


Fig. 2. Various pKa of amino acids Alanine, Aspartic acid, and Lysine and charge distributions under different pH values. In the upper panel, the numbers indicate various pKa values including the side chains for Aspartic acid and Lysine. Since Alanine side chain has no charge, it only has a methyl group, so there is only 2 pKa. The lower panel, the range of charged side chains. +2, +1, 0, -1, and -2 indicate the net charges the peptides bear. Dark blue: +2 charge, light blue: +1 charge, green: 0 charge, pink: -1 charge, and red: -2 charge.

2.2. Dynamic Light Scattering (DLS)

Light scattering is one of the convenient methods to determine CAC.²⁴ DLS intensity correlates with the aggregation sizes. Below CAC, there are mostly monomer and small clusters, too small to be undetectable by the instrument. When the monomer and cluster starts to assemble, the intensity in DLS undergo exponentially increase as function of concentration increase. The same behavior was shown in Figure 3. The intensity in DLS was negligible when the concentration is below the CAC, and varied gradually near the CAC. As soon as it crosses the CAC threshold, the intensity undergoes dramatic change indicating the formation of large assembled structures. The DLS results showed that A₆D and A₆K have characteristics as typical surfactants, self-assembly driven mostly from hydrophobic interaction. The gradual increase of intensity near CAC suggested that assembly was not typical alkyl tail hydrophobic interaction, but less strong

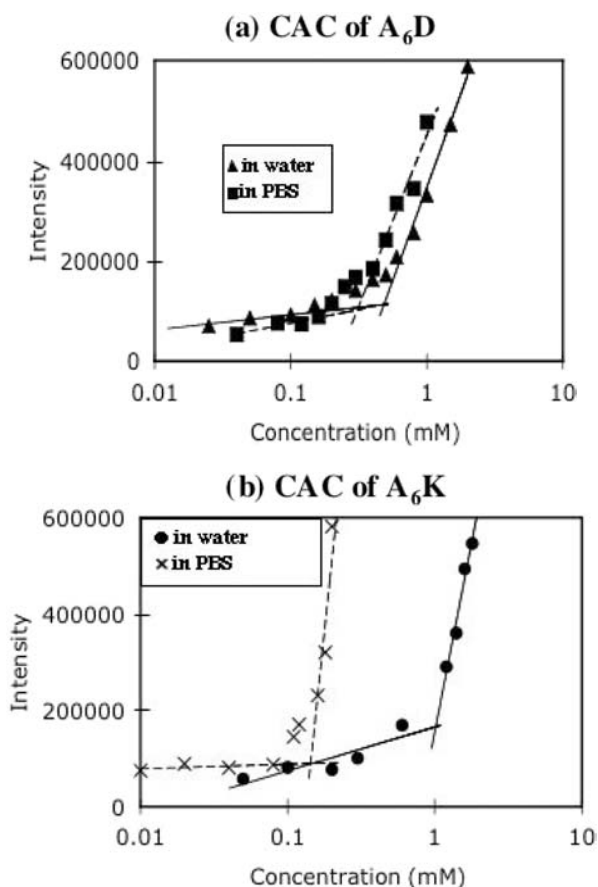


Fig. 3. Critical aggregation concentration (CAC) determination in water and phosphate-based saline (PBS, 150 mM NaCl/10 mM Na-PO₄): (a) A₆D. The *x* axis is the concentration of peptides, and the *y* axis is the intensity in dynamic light scattering (DLS). The CAC value was estimated by the intersection of the two linear regression lines. The CAC were indicated below: 0.46 mM (A₆D in water), 0.3 mM (A₆D in PBS). (b) A₆K, 1.02 mM (A₆K in water), 0.14 mM (A₆K in PBS). The CAC value, especially of A₆K, dramatically changed due to ionic strength in PBS.

hydrophobic interaction for the tails. The solutions of these peptides were also poly-dispersed suggesting variation of assembled nano-structures. However DLS cannot quantitatively determine numbers of assemblies because it cannot distinguish the structures between micelles and vesicles.

The CAC differences of the assembled peptides in Milli-Q pure water solution and PBS solution were also observed in DLS in Figure 3. These measured CAC were as follows: 0.46 mM (A₆D in water), 0.3 mM (A₆D in PBS), 1.02 mM (A₆K in water), 0.14 mM (A₆K in PBS). The CAC of peptides in PBS were lower than that in water since PBS contain salt. This reduction in CAC in PBS salt solution is mainly due to the decrease in electrical repulsion between the ionic head-groups. Furthermore salt ions interact with water thus reducing the number of water molecules to hydrate peptides. These observations suggested that the CAC of each peptide varies depending on the solution environment including salts. It is important to emphasize, in biochemical experiments, all solutions contain salt including PBS solution. Thus, knowing each CAC is very important to dissolve hydrophobic substances especially membrane proteins. Thus the CAC in PBS for lipid-like peptides need to be determined for biology experiments.

2.3. Atomic Force Microscopy (AFM)

In order to experimental observe the dynamic structural behaviors of the lipid-like peptides A₆D and A₆K, AFM was used to follow their structures. AFM is useful tool to observe the structure in very fine details with minimal sample disturbance since there is no sample treatment except load it onto the mica surface.

From the dynamic light scattering results of various peptide concentrations, the peptide assemblies were poly-dispersed with different size and form of assemblies. Thus, peptide concentrations ranging from 0.04 mM to 6 mM of A₆D solutions were used to acquire images of the assemblies. The PBS solutions of A₆D were used for AFM measurement. Since mica surface is negatively charged, so counter ions between A₆D molecules, which also have negative charges, are necessary to allow A₆D peptides to attach on mica surface. Several types of nanostructures were observed above 0.3 mM (Fig. 4). At 0.04 mM of which intensity in DLS was lower than CAC, no apparent nano-structures were observed. Although CAC was 0.3 mM in PBS solution, intensity in DLS started increasing ~0.3 mM of which AFM image already showed spherical assemblies. At 0.5 mM, other structure were observed, they become wider and longer as a function of peptide concentration increase.

Interestingly unusual structures of the nanotube with regular bulges were observed in 4.0 mM and 6.0 mM of A₆D solutions. The AFM images not only revealed

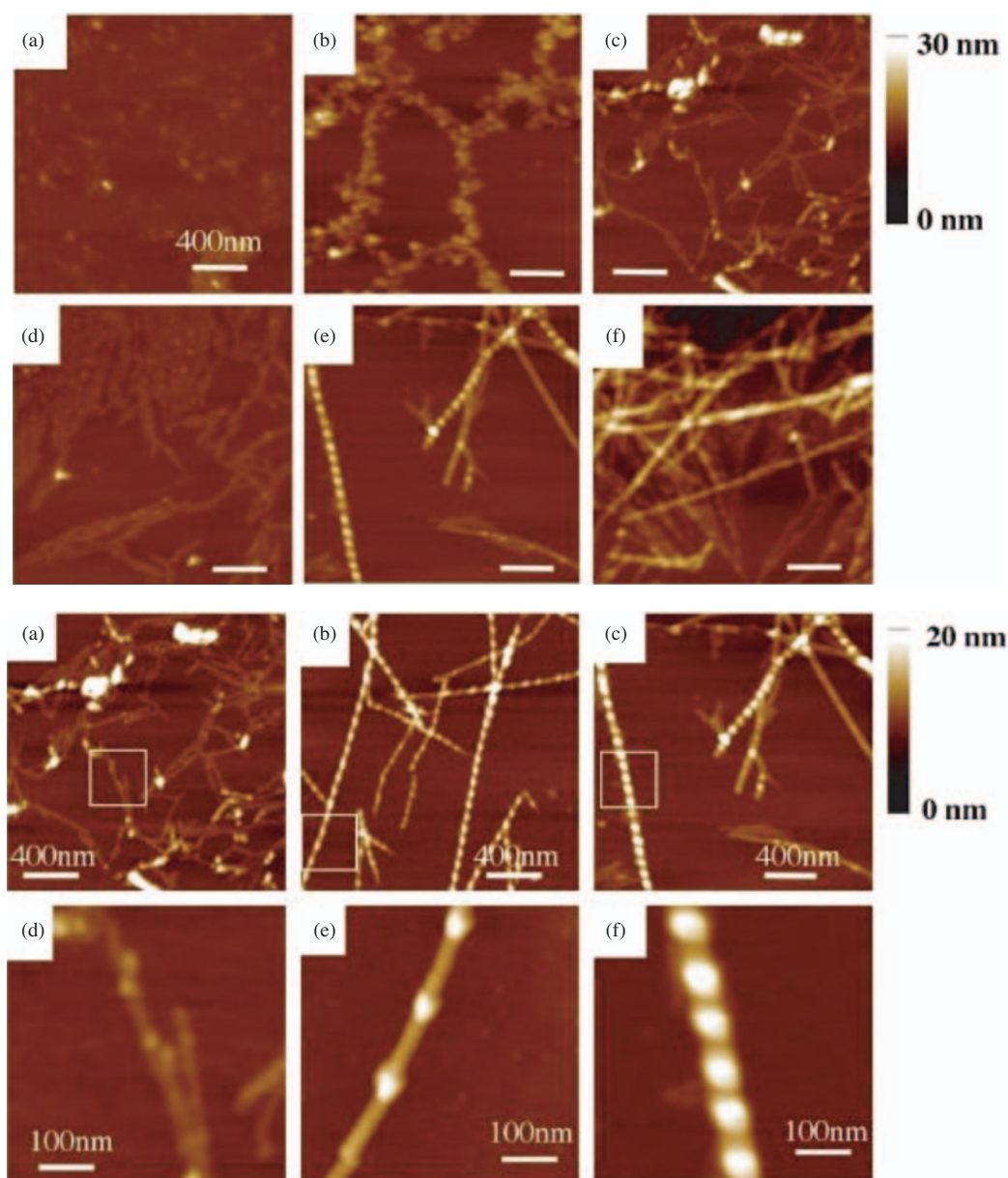


Fig. 4. AFM images of nanostructures of A₆D lipid-like self-assembling peptides. Upper panel: A₆D, (a) 0.04 mM; (b) 0.3 mM; (c) 0.5 mM; (d) 1.0 mM; (e) 4.0 mM; (f) 6.0 mM. Spherical aggregations were observed at the CAC (0.3 mM). The aggregation transformed into nanotubes becoming thicker and longer as a function of A₆D concentration increase above its CAC. Particularly, a unique shape of the nanofiber with repeated bulges were observed in 4.0 mM and 6.0 mM of A₆D solutions. Each scale bar represents 400 nm. Lower panel: AFM images of the A₆D nanotubes. (a) 0.5 mM; (b) 2 mM; (c) 4 mM; (d–f) enlarged image of (a–c), respectively. The A₆D nanotubes changed as a function of A₆D concentration increase. The bundles of thin nanotubes were observed in relatively low concentration (0.5 mM). The nanotube appeared at 2.0 mM. The pitch between the bulges reduced. A thick nanotubes with the bulges were observed at 4.0 mM.

the forms and sizes of structures but also their dynamic changes depending on concentrations of A₆D. These results also correlated with the peptide solution intensity increasing determined in DLS. These elongated assemblies rather than spherical assemblies seemed to contribute to intensity in DLS. To observe details of assemblies, enlarged images were shown in Figure 4. The structures of the assemblies in A₆D solution transformed as a result of the increase in A₆D concentration. The bundles of nanotubes were also observed in low concentration

(0.5 mM). The nanotubes with bulges at regular interval appeared at ~2.0 mM. The apparent helical pitch between the bulges became shorter and wider at 4.0 mM (Fig. 4 lower panel, c and f).

2.4. Molecular Modeling

The observed peptide nanostructures are similar as previous studies.^{21–24} However, in this report, we systematically studied different structures at different peptide

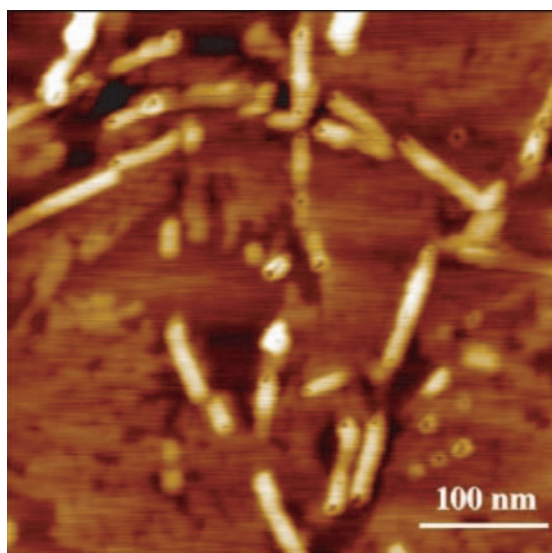


Fig. 5. The AFM image of nanotubes of A₆K lipid-like self-assembling peptides. When the peptide solution pH is less than the Lysine pK_a 10, the peptide bears a positive charge. The openings of peptide nanotubes are clearly visible. These nanotube structures can also undergo structural changes depending on various conditions, particularly pH changes, ionic strength of salts, temperature and incubation time. The other sheets like materials are likely the un-assembled peptides at the time of the image collected.

concentrations. The phenomena are similar as many surfactants behavior. It is well known that there are several structural transitions from spherical micelles to cylindrical micelles, lamellar micelles, etc, as the concentration of surfactant is increased.

From available information, we here propose a schematic illustration of the peptide assembly structures at different concentrations (Fig. 6). Below the CAC, small assemblies such as micelles or vesicle are formed. As the peptide concentration increase, structural transitions of the assemblies take place above CAC of the lipid-like peptides in both water and PBS. There exist single nanotube structure, bundles of nanotubes, and wider nanotubes with the regular pitches of multiple bulges. In this proposed model, nanotubes and bundle of nanotubes with the bulges are reversible. The diameter changes would be related to packing densities of vesicle tubes. Although a full computational molecular modeling is beyond our current capability, we propose a plausible path of self-assembly for the nanotubes and other nanostructures observed in our experiments.

The main purpose of our current systematic study of the lipid-like peptides is to tackle the challenging problems of membrane protein solubilization, stabilization, and crystallization. Since membrane proteins themselves are Nature-made nanomachines and nanodevices, our systematic study such lipid-like peptides will likely contribute to further study of the intractable membrane proteins. This class of designer lipid-like peptides is readily for large-scale synthesis at reasonably cost, amenable to high-throughput

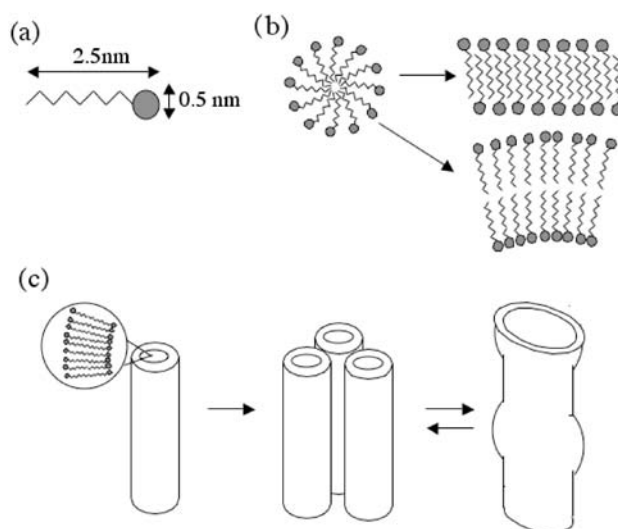


Fig. 6. A proposed schematic illustration of dynamics of nanostructural transitions of numerous lipid-like self-assembling peptides: (a) A single lipid-like peptide monomer with hydrophilic head and hydrophobic tail. The approximate 2.5 nm length is similar as common lipids found in cell membranes. (b) Self-assembly of numerous peptides to form micelle and other simpler structures above the CAC of the lipid-like peptides. It is plausible that the hydrophobic peptide tail packing, both anti-parallel and parallel is possible, similar as found in anti-parallel and parallel beta-sheet packing. (c) Dynamic structural transition behaviors in various assemblies above CAC, for example, a single peptide nanotube, a bundle of nanotubes, and dynamically fused tubes bulge, observed under AFM and TEM previously. Since the nanotube structures are made through numerous individual lipid-like self-assembling peptides through weak interactions, hydrogen bonds and hydrophobic interactions, the coalesced tubes between last two steps may be dynamically reversible as schematically illustrated here.

structural screening as well as for other wide spread uses in nanoscience and nanobiotechnology.

Acknowledgments: We thank members in of our laboratory for helpful and stimulating discussions. This work is supported in part by grants from the Multidisciplinary University Research Initiative (MURI)/AFOSR, and the National Science Foundation to the Center for Bits and Atoms to the Massachusetts Institute of Technology.

References and Notes

1. S. Zhang, *Nature Biotechnology* 21, 1171 (2003).
2. R. Langer and D. Tirrell, *Nature* 428, 487 (2004).
3. A. Aggeli, M. Bell, N. Boden, J. N. Keen, P. F. Knowles, T. C. B. Mcleish, M. Pitkeathly, and S. E. Radford *Nature* 386, 259 (1997).
4. M. Reches and E. Gazit, *Science* 300, 625 (2003).
5. M. R. Ghadiri, J. R. Granja, and L. K. Buehler, *Nature* 369, 301 (1994).
6. M. W. West, W. Wang, J. Patterson, J. D. Mancias, J. R. Beasley, and M. H. Hecht, *Proc. Natl. Acad. Sci. USA* 96, 11211 (1999).
7. M. S. Lamm, K. Rajagopal, J. P. Schneider, and D. J. Pochan *J. Am. Chem. Soc.* 127, 16692 (2005).
8. T. Scheibel, R. Parthasarathy, G. Sawicki, X. M. Lin, H. Jaeger, and S. L. Lindquist, *Proc. Natl. Acad. Sci. USA*
9. M. G. Ryadnov and D. N. Woolfson, *Nature Mater.* 2, 329 (2003).

10. S. Toledano, R. J. Williams, V. Jayawarna, and R. V. Ulijn, *J. Am. Chem. Soc.* 128, 1070, (2006).
11. M. Biesalski, A. Knabel, R. Tu, and M. Tirrell, *Biomaterials* 27, 1259 (2006).
12. J. M. Schnur, *Science* 262, 1669 (1993).
13. Y. M. Lvov, R. R. Price, J. V. Selinger, A. Singh, M. S. Spector, and J. M. Schnur, *Langmuir* 16, 5932 (2000).
14. M. S. Spector, A. Singh, P. B. Messersmith, and J. M. Schnur, *Nano Lett.* 1, 375 (2001).
15. S. Zhang, T. Holmes, C. Lockshin, and A. Rich, *Proc. Natl. Acad. Sci. USA* 90, 3334 (1993).
16. S. Zhang, T. Holmes, M. DiPersio, R. O. Hynes, X. Su, and A. Rich, *Biomaterials* 13, 1385 (1995).
17. T. Holmes, S. Delacalle, X. Su, A. Rich, and S. Zhang, *Proc. Natl. Acad. Sci. USA* 97, 6728 (2000).
18. S. Zhang, F. Gelain, and X. Zhao, *Seminars in Cancer Biology* 15, 413 (2005).
19. D. Marini, W. Hwang, D. A. Lauffenburger, S. Zhang, and R. D. Kamm, *Nano Lett.* 2, 295 (2002).
20. S. Zhang, L. Yan, M. Altman, M. Lassle, H. Nugent, F. Frankel, D. A. Lauffenburger, G. Whitesides, and A. Rich, *Biomaterials* 20, 1213 (1999).
21. S. Vauthey, S. Santoso, H. Gong, N. Watson, and S. Zhang, *Proc. Natl. Acad. Sci. USA* 99, 5335 (2002).
22. S. Santoso, W. Hwang, H. Hartman, and S. Zhang, *Nano Lett.* 2, 687 (2002).
23. G. Von Maltzahn, S. Vauthey, S. Santoso, and S. Zhang, *Langmuir* 19, 4332 (2003).
24. S. Yang and S. Zhang, *Supramolecular Chemistry* 18, 389 (2006).
25. M. R. Ghadiri, J. R. Granja, R. A. Milligan, D. E. McRee, and N. Khazanovich, *Nature* 366, 324 (1993).
26. S. Fernandez-Lopez, H. S. Kim, E. C. Choi, M. Delgado, J. R. Granja, A. Khasanov, K. Kraehenbuehl, G. Long, D. A. Weinberger, K. M. Wilcoxon, and M. R. Ghadiri, *Nature* 412, 452 (2001).
27. O. Carny, D. Shalev, and E. Gazit, *Nano Lett.* 6 (2006), (in press).
28. E. Wallin and G. von Heijne, *Protein Science* 7, 1029 (1998).
29. P. J. Loll, *J. Struct. Biol.* 142, 144 (2003).
30. P. J. Kiley, X. Zhao, M. Vaughn, M. Baldo, B. D. Bruce, and S. Zhang, *PLoS Biol.* 3, 1181 (2005).
31. J. I. Yeh, S. Du, A. Tordajada, J. Paulo, and S. Zhang, *Biochemistry* 44, 16912 (2005).
32. X. Zhao, Y. Nagai, P. Revees, P. Kiley, H. G. Khorana, and S. Zhang, *Proc. Natl. Acad. Sci. USA* 103 (2006), (in press).

Received: xx Xxxx xxxx. Accepted: xx Xxxx xxxx.